A molecular dynamics quantum Kramers study of proton transfer in solution

Dimitri Antoniou and Steven D. Schwartz

Citation: The Journal of Chemical Physics **110**, 465 (1999); doi: 10.1063/1.478107
View online: http://dx.doi.org/10.1063/1.478107
View Table of Contents: http://scitation.aip.org/content/aip/journal/jcp/110/1?ver=pdfcov
Published by the AIP Publishing

A molecular dynamics quantum Kramers study of proton transfer in solution

Dimitri Antoniou and Steven D. Schwartz
Department of Physiology and Biophysics, Albert Einstein College of Medicine, Bronx, New York 10461

(Received 9 June 1998; accepted 29 September 1998)

We present a quantum study of a proton transfer reaction $AH{-}B \rightleftharpoons A^{-}{-}H^{+}B$ in liquid methyl chloride, where the AH–B complex corresponds to phenol-amine. We use the same intramolecular potentials that were used in two earlier studies of this system [H. Azzouzz and D. Borgis, J. Chem. Phys. **98**, 7361 (1993); S. Hammes-Schiffer and J. C. Tully, J. Chem. Phys. **101**, 4657 (1994).] The former study employed a Landau-Zener approach and a molecular dynamics centroid method, while the latter a surface-hopping method. These studies obtained results that differ by an order of magnitude. In the present work, we first performed a molecular dynamics simulation to obtain the spectral density, which was then used as an input to the method we have developed for the study of the quantum Kramers problem [S. D. Schwartz, J. Chem. Phys. **105**, 6871 (1996)]. Thus, in this work both the reaction coordinate and the bath are treated quantum mechanically.
 [S0021-9606(99)52101-6]

I. INTRODUCTION

The theoretical study of reaction rates in a condensed phase is one of the central problems in chemical physics. However, the details of the interactions between the reaction coordinate, the solvent and nonreactive modes are unknown even for very simple systems. For this reason, many researchers have focused their attention on simple phenomenological models that have been found to be useful in the interpretation of experimental results. For example, an extremely useful model of classical activated barrier crossing in solution is the generalized Langevin equation (GLE)

$$m_s\ddot{s} = -\frac{\partial V(s)}{\partial s} + \int_0^t dt'\,\gamma(t-t')\dot{s} + F(t), \tag{1.1}$$

where $V(s)$ is the potential along the reaction coordinate s, $F(t)$ is the fluctuating force of the environment and $\gamma(t)$ is the dynamical friction which obeys the fluctuation-dissipation theorem[1]

$$\gamma(t) = \frac{1}{k_B T}\langle F(0)e^{-iQLt}F(0)\rangle, \tag{1.2}$$

where L is the Liouville operator and the operator Q projects[1,2] onto the orthogonal complement of $\dot{s}$ (there are good arguments[3,4] that suggest that it is a good approximation to replace $e^{-iQLt}F(0)$ by the force $F(t)$ calculated while holding the reaction coordinate fixed at the top of the barrier).

The theory of activated transfer in a condensed phase was developed as a microscopic theory with the observation[5] by Zwanzig that when the classical Hamiltonian

$$H = \frac{P_s^2}{2m_s} + U(s) + \sum_k \left[\frac{P_k^2}{2m_k} + \frac{1}{2}m_k\omega_k^2\left(q_k - \frac{c_k s}{m_k\omega_k^2}\right)^2\right] \tag{1.3}$$

is integrated in the bath coordinates, it produces the Generalized Langevin Equation Eq. (1.1). This statement is nontrivial once we realize that it implies that integration of Eq. (1.3) leads to an equation that describes phenomena that are irreversible in time. In Sec. IV we shall see that the Hamiltonian Eq. (1.3) provides a natural starting point for a quantum calculation.

The dynamical friction $\gamma(t)$ can be expressed in terms of the microscopic coefficients c_k, m_k, ω_k that appear in Eq. (1.3) in the following manner:

$$\gamma(t) = \sum_k \frac{c_k^2}{m_k\omega_k^2}\cos(\omega_k t), \tag{1.4}$$

for a discrete bath, while a similar expression holds for an infinite bath. If we assume, as is often the case, that $\gamma(t)$ is independent of temperature and the position x, then the solution of the GLE Eq. (1.1) depends only on $\gamma(t)$ and not on the particular set of parameters c_k, m_k, ω_k that generate it through Eq. (1.4). The dynamical friction $\gamma(t)$ leads directly to a quantity that is experimentally observable in reaction rate measurements. Grote and Hynes[6] used the GLE to find corrections to the transition state theory rate k_{TST}:

$$k_{\mathrm{GH}} = \frac{\lambda_0^{\neq}}{\omega_b}k_{\mathrm{TST}}, \tag{1.5}$$

where ω_b is the reactive barrier frequency; in the strong friction limit the Grote-Hynes coefficient $\lambda_0^{\neq}/\omega_b$ is the solution of the integral equation

$$\frac{\lambda_0^{\neq}}{\omega_b} = \frac{\omega_b}{\lambda_0^{\neq} + \hat{\gamma}(\lambda_0^{\neq})}, \tag{1.6}$$

where

$$\hat{\gamma}(\lambda_0^{\neq}) = \int_0^{\infty} dt e^{-\lambda_0^{\neq} t}\gamma(t), \tag{1.7}$$

is the Laplace transform of the dynamical friction. The case of Markovian hopping corresponds to $\gamma(t)=2\eta\delta(t)$, which leads to $\hat{\gamma}(\lambda_0^{\neq})=2\eta$.

Many experimental studies have confirmed the validity of Grote-Hynes theory, and as a consequence, of the GLE as an accurate phenomenological description of activated reactions in solution. This success has led to a widely adopted scheme for performing classical simulations[7,8] of realistic models of reactions in solution: define some intramolecular potential, use molecular dynamics to calculate the force-force correlation function and finally using Eq. (1.2) calculate the dynamical friction. Then one can calculate the Grote-Hynes factor Eq. (1.6). In Sec. IV we shall see how a similar scheme can be used for the calculation of the spectral density, which is then used as an input for a quantum calculation. Until very recently it was not feasible to use such a detailed description for a quantum reaction coordinate in a quantum condensed phase environment.

Thus, there has been significant effort in the past 10 years aimed at the development of accurate but approximate quantum treatments of reaction in a condensed phase. Three highly significant efforts at such formulations are the Landau-Zener curve hopping approach of Borgis and Hynes,[9] the effective potential centroid methods applied in the same work,[10,11] and the molecular dynamics with quantum transitions method developed in Tully's group.[12] Azzouzz and Borgis applied[13] both the Landau-Zener formulation and the centroid method to a model of proton transfer in methyl chloride. Tully then applied[14] the surface hopping method to the same potential. Numerically different results from the two groups studies were obtained. In this paper we apply our recently developed quantum operator methods to calculate the rate of proton transfer in the same model via a quantum activated rate study.

The structure of the remainder of this paper is as follows: in the next section we shall describe the intramolecular potentials that were constructed by Azzouzz and Borgis for the simulation of a proton transfer reaction in liquid methyl chloride. In Sec. III we shall briefly review the quantum calculations of this system that were performed in Refs. 13, 14. Finally, in Sec. IV we shall perform a quantum calculation that draws from our previous work on the quantum Kramers problem.[15,16] The results from the variety of approaches will then be compared. The paper closes with a discussion of the results and possible extensions to the calculations.

II. INTERMOLECULAR POTENTIALS

The model system we will be studying is the proton transfer reaction $AH{-}B \rightleftharpoons A^{-}{-}H^{+}B$ in liquid methyl chloride. We are using a linear model for the AH–B complex with parameters chosen to model a phenol-amine complex (i.e., A and B stand for ΦO and NR_3, respectively). The complex can be found in either a covalent (AH–B) or an ionic (A^{-}–H^{+}B) form. The total potential energy can be written as a sum of three terms:

$$V=V_{\text{compl}}+V_{\text{solv}}+V_{\text{compl-solv}}. \tag{2.1}$$

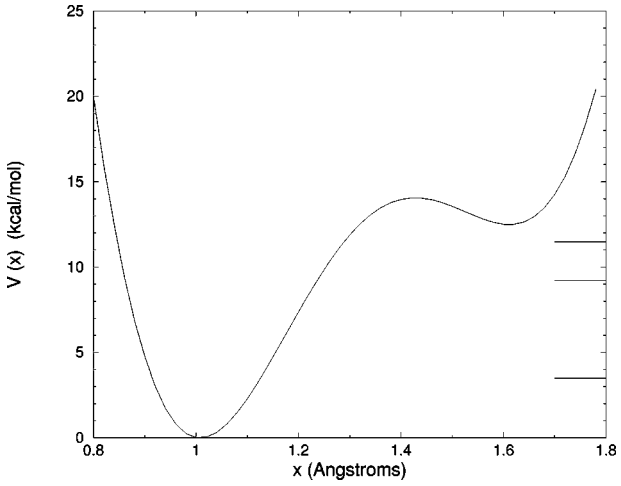

FIG. 1. The potential energy surface Eq. (2.2). The lowest three eigenvalues are also shown on the right-hand side; see the discussion in Sec. IV.

The first term is the H-bonding interaction within the complex, the second term describes interactions between the solvent molecules and the third term represents interactions between the complex and solvent molecules. Azzouzz and Borgis[13] constructed these potentials in the following fashion.

A. Complex potential

Define R as the distance between the A, B groups (both are modeled as single sites) of the complex AH–B and x the distance between A and H. Then the hydrogen bonding interaction within the complex takes the following form:

$$V_{\text{compl}}=be^{-aR}+D_{\text{A}}[1-e^{-n_{\text{A}}(x-d_{\text{A}})^2/2x}] + cD_{\text{A}}[1-e^{-n_{\text{B}}(R-x-d_{\text{B}})^2/2(R-x)}]. \tag{2.2}$$

The first term is a core repulsion between A and B, while the last two terms represent chemical bonding of H with A and B respectively, in a functional form introduced by Lippincott and Schröder.[17] The choice of various parameters in Eq. (2.2) is the following (these values correspond to model II of Ref. 13):

(i) D_{A} is taken to be the dissociation energy of OH bonds in gas phase, $D_{\text{A}}=D_{\text{OH}}=110$ kcal/mol.
(ii) $c=0.776$ was chosen to allow for stabilization of the ionic complex in methyl-chloride.
(iii) $d_{\text{A,B}}$ and $n_{\text{A,B}}$ are fixed by, respectively, the equilibrium bond distance and vibrational frequency modes ($\omega_{\text{OH}}=3650\ \text{cm}^{-1}$, $\omega_{\text{NH}}=3550\ \text{cm}^{-1}$) in the gas phase: $d_{\text{A}}=d_{\text{OH}}=0.95$ Å, $d_{\text{B}}=d_{\text{NH}}=0.97$ Å, $n_{\text{A}}=9.26\ \text{Å}^{-1}$, and $n_{\text{B}}=11.42\ \text{Å}^{-1}$.

In Fig. 1 we plot the potential Eq. (2.2) for the AB distance $R=2.7$ Å. This corresponds to a H–N bond of intermediate strength.[13] The zero of the potential energy was taken at the minimum of the potential.

B. Solvent potential

The CH_3Cl molecule is modeled as a two-site potential, i.e., the methyl group is reduced to a single atomic site. If m,n label different solvent molecules and $i(j)$ different sites in the mth (nth) molecule, then the solvent-solvent interaction is given by

$$V_{mn}=\sum_{i\in m}\sum_{j\in n}\left[\frac{q_iq_j}{r_{ij}}+\frac{A_iA_j}{r_{ij}^{12}}-\frac{C_iC_j}{r_{ij}^{6}}\right], \tag{2.3}$$

i.e. the solvent-solvent interaction has a Coulomb and a Lennard-Jones component. The parameters in Eq. (2.3) are taken from the Monte Carlo simulations of Bigot:[18]

(i) CH_3 site: $q/e=0.25$, $A^2=7.95\times10^6$ Å^{12} kcal/mol, $C^2=2750$ Å^6 kcal/mol.

(ii) Cl site: $q/e=-0.25$, $A^2=5.25\times10^6$ Å^{12} kcal/mol, $C^2=2950$ Å^6 kcal/mol.

C. Complex-solvent potential

We have to distinguish between the Lennard-Jones and the Coulombic components of the complex-solvent interaction.

Lennard-Jones: The A and B groups of the complex interact with the methyl and chloride sites of the solvent molecule through a Lennard-Jones force with parameters

$$\sigma=3.5\ \text{Å} \quad \text{and} \quad \epsilon=200\ \text{K}. \tag{2.4}$$

Coulomb: The sites in the solvent molecule interact with point charges e_α in the complex where $\alpha=$A,H,B. The Azzouzz–Borgis model allows for the variation of charge distribution as the complex evolves from a covalent to an ionic state, in the following manner:

$$e_\alpha=(1-f\ )e_\alpha^{\text{covalent}}+fe_\alpha^{\text{ionic}}(\alpha=\text{A,H,B}),$$

$$f=\frac{1}{2}\left[1+\frac{x-x_0}{\sqrt{(x-x_0)^2+l^2}}\right], \tag{2.5}$$

where $x_0=1.43$ Å is the position of the barrier top for the gas-phase potential shown in Fig. 1 and $l=0.125$ Å.

The covalent (reactant) state is defined by

$$e_{\text{A}}^{\text{covalent}}=-0.5e,\quad e_{\text{H}}^{\text{covalent}}=+0.5e,\quad e_{\text{B}}^{\text{covalent}}=0e \tag{2.6}$$

and the ionic (product) state by

$$e_{\text{A}}^{\text{ionic}}=-1.0e,\quad e_{\text{H}}^{\text{ionic}}=+0.5e,\quad e_{\text{B}}^{\text{ionic}}=0.5e, \tag{2.7}$$

(these values correspond to a dipole moment $\mu=2.5$ D). Before we proceed, we should point out that these model potentials do not include the electronic polarization part of either the complex or solvent.[13]

III. ALTERNATIVE QUANTUM RATE CALCULATIONS

In this section we shall briefly outline three quantum rate calculations for the system described in Sec. II. The first two were performed by Azzouzz and Borgis[13] and the last one by Hammes-Schiffer and Tully.[14] The first two are in approximate agreement with each other, the third one predicts a rate that is one order of magnitude larger and a kinetic isotope effect that is one order of magnitude smaller than the earlier result.

A. Curve-crossing calculation

Azzouzz and Borgis performed a molecular dynamics (MD) simulation and calculated the force exerted by the solvent on the complex internal coordinates. Then, the solvation free energy was calculated and added to the complex potential Eq. (2.1) in order to obtain an effective potential energy surface $W(r)$ for the proton. Remarkably, they found that (for $R=2.7$ Å) the stabilization of the solvent reduces the energy gap between the covalent and ionic states to only 1 kcal/mol, even though the energetic barrier remains high, approximately 12 kcal/mol. Since the barrier of the effective potential $W(r)$ is very high, Azzouzz and Borgis made a reasonable assumption that a two-level approximation is adequate. For the calculation of the rate they used an approach developed by Borgis and Hynes,[9] whose basic idea is that the quantum hopping is described as a Landau-Zener curve-crossing process. These assumptions are nontrivial if we recall that the effective potential $W(r)$ was calculated after averaging *classical* trajectories for the solvent molecules and was then used for the study of the *quantum* dynamics of the reaction coordinate x. We refer the reader to Ref. 13 for details of the calculation. The final result for the rate was $k=7.8\times10^9$ s^{-1} and a KIE equal to 46.

B. Centroid method

Azzouzz and Borgis calculated the rate by an independent method in order to check their curve-crossing calculation. In particular, they used a molecular dynamics version of the centroid method. Some applications of the centroid method are listed in Ref. 10 while a review can be found in Ref. 11. Azzouzz and Borgis used their molecular dynamics calculation in order to calculate the effective potential energy surface $W(\xi)$ for the centroid ξ of the proton thermal path. Details of the calculation can be found in Ref. 13. The rate was found to be equal to 10.5×10^9 s^{-1} and the KIE equal to 40. These values are in good agreement with the results of the curve-crossing calculation.

C. Molecular dynamics with quantum transitions

A quite different approach to the study of quantum dynamics in systems with many degrees of freedom, is taken in ''surface hopping'' methods.[19] In these methods there is a separation into the quantum reaction coordinate x and the presumed classical solvent degrees of freedom Q. The delicate problem with such mixed quantum-classical methods is the following. The classical degrees of freedom follow some trajectory $Q(t)$, while the reaction coordinate x might switch between different quantum states. Since $Q(t)$ is coupled to the quantum coordinate, a consistent calculation should require $Q(t)$ to switch, too, to a different classical trajectory. Of course, this cannot happen within the Newtonian equations of motion. The surface-hopping methods provide a rule

that determines if such switches should occur between quantum states and as a consequence, between classical trajectories.

There are several implementations of surface-hopping methods. Tully has developed a method[12] that is based on a ''fewest switches'' algorithm. This algorithm was applied on the Azzouzz–Borgis model in Ref. 14. We only cite the final result of that calculation: a rate equal to 78×10^{10} s^{-1} and a KIE equal to 3.9. The rate is one order of magnitude larger than the result of Azzouzz–Borgis while the KIE is one order of magnitude smaller.[20]

IV. QUANTUM KRAMERS CALCULATION

In the previous section we briefly discussed some of the most successful modern theories of reaction rates in condensed phases that attempt a realistic description of the bath. These methods when applied to the same model gave results that differ by an order of magnitude. It is difficult to decide which result is accurate since all three methods employ different approximations for the description of the interplay of the quantum dynamics of the reaction coordinate and the bath.

In this paper we shall adopt an alternative strategy for the calculation of activated rates in a solvent that is described by some realistic model. This method is a direct extension of our previous work on the quantum Kramers problem.[15,16]

The form of Eq. (1.3) allows a straightforward generalization to the quantum case, by treating the bath oscillators quantum-mechanically. At first sight, the task of solving Eq. (1.3) appears hopeless since we need to know the parameters c_k, m_k, ω_k for all the bath modes. Fortunately, if the dynamical friction $\gamma(t)$ that appears in Eq. (1.1) is independent of position and temperature, the influence of the bath on the dynamics is determined only by the spectral density

$$J(\omega)=\frac{\pi}{2}\sum_k \frac{c_k^2}{m_k\omega_k}\,\delta(\omega-\omega_k). \tag{4.1}$$

When the bath is infinite, $J(\omega)$ becomes a continuous function of the mode frequency ω. For a *harmonic* bath there is a simple relation[5] between the spectral density and the dynamical friction of the corresponding Generalized Langevin Equation

$$\gamma(t)=\int_0^\infty d\omega\,\frac{J(\omega)}{\omega}\cos(\omega t). \tag{4.2}$$

The Markovian case $\gamma(t)=2\eta\delta(t)$ corresponds to an ''Ohmic'' spectral density $J(\omega)=\eta\omega$. Since a real finite bath has an upper limit for the frequency of its normal modes, it is common to add an exponential cutoff, i.e., the spectral density becomes

$$\eta\omega e^{-\omega/\omega_c}. \tag{4.3}$$

If the thermal energy $k_BT>\omega_c$, then most of the bath modes are excited and the bath behaves classically. Then if we use a molecular dynamics simulation to find the spectral density $J(\omega)$, we can approximate the quantum spectral density by its classical counterpart. This is the reason many workers include in their quantum calculation a spectral density that was derived by a classical simulation.

TABLE I. Comparison of the ratio k/k_{ZPE} of the quantum rate k over k_{ZPE}, which is the TST result corrected for zero-point energy in the reactant well, as calculated in the present paper (with a gas-phase and a mean field potential) and in Ref. 13 (Landau-Zener and centroid methods) and Ref. 14 (molecular dynamics with quantum transitions).

This work (MFP)	This work (gas-phase)	Ref. 13 (LZ)	Ref. 13 (centroid)	Ref. 14 (MDQT)
75	1150	907	1221	9080

In order to map the dynamics onto the GLE Eq. (1.1) we need to know the mean-field potential $U(s)$. Let us recall the way the mean-field potential enters the Zwanzig Hamiltonian Eq. (1.3). If $V(s)$ is the bare potential, then the total potential energy is

$$V(s)+\sum_k\left(\frac{1}{2}m_k\omega_k^2q_k^2-cq_ks\right). \tag{4.4}$$

In order to bring this into the form of the potential energy of Eq. (1.3), we have to complete the square in the second term:

$$\left[V(s)-\sum_k\frac{c_ks^2}{2m_k\omega_k^2}\right]+\sum_k\frac{1}{2}m_k\omega_k^2\left(q_k-\frac{c_ks}{m_k\omega_k^2}\right)^2. \tag{4.5}$$

The first term is the mean-field potential $U(s)$ that appears in the Zwanzig Hamiltonian Eq. (1.3). When the bare potential $V(s)$ has a double-well form, then U(s) is the ''adiabatic'' potential[21] along the minimum energy path. However, it is not necessarily the adiabatic potential U(s) that is the relevant potential barrier for the transfer reaction.

In particular,[21] the reaction coordinate does follow a trajectory close to the minimum energy path in the ''adiabatic'' limit, when the bath is fast compared to the motion of the reaction coordinate. However, in the opposite ''fast-flip'' limit, the reaction coordinate will follow a trajectory close to the static barrier (see Fig. 17 of Ref. 21).

For the system examined in the present paper, we shall shortly find in the discussion of the calculated spectral density, that the response of the bath is very slow compared to the fast tunneling motion of the proton, therefore the latter ''fast-flip'' limit is relevant. It would seem then that in the Zwanzig Hamiltonian the potential U(x) should be set equal to the gas phase potential Eq. (2.2). We have computed the rates for both the gas phase potential and potential of mean force and present the results below (see Table I). From Eq. (4.5) it is clear that the mean-field potential has a higher barrier and as a result the rate is lower.

The procedure we will follow for the calculation of the quantum rate in the system described in Sec. II is the following:

(i) Perform a molecular dynamics simulation and calculate the force-force correlation function, i.e., the dynamical friction $\gamma(t)$.
(ii) Evaluate the cosine Fourier transform Eq. (4.2) in order to find the spectral density $J(\omega)$.

(iii) Solve the quantum Kramers problem that has a spectral density equal to the one calculated in step (ii).

This scheme has been used before in quantum calculations, for example in the works cited in Ref. 22. The justification for this approach is as follows: the dynamics of the linear GLE is completely determined by the dynamical friction $\gamma(t)$. If a harmonic bath that is bilinearly coupled to the reaction coordinate has a spectral density that corresponds through Eq. (4.2) to a dynamical friction that is identical to the one that was derived through the molecular dynamics simulation, then the dynamics of a particle that is bilinearly coupled to this *hypothetical* harmonic bath is identical to the dynamics of a particle coupled to the real anharmonic bath, if the system is well described by the linear GLE. This is the crucial point about the Zwanzig Hamiltonian Eq. (1.3): the harmonic modes appearing there, need no bear any relation to the modes of the actual solvent; the only requirement is that Eq. (1.4) must generate the correct dynamical friction.

We shall repeat the assumptions that are implicit in the scheme we are adopting:

(i) The classical dynamics of the charge transfer can be described by a linear GLE, so that the resulting dynamic friction is independent of position and temperature.
(ii) Most of the solvent modes have low frequency, so that they are thermally excited.
(iii) We use a quantum generalization of the Zwanzig Hamiltonian Eq. (1.3); the bath is described quantum mechanically and has a spectral density that is approximated by the spectral density of a hypothetical classical harmonic bath.

A. Molecular dynamics simulation

We used the intermolecular potentials described in Sec. II. Following Refs. 13 and 14 we used in our simulation periodic boundary conditions in a cubic box of length 28 Å for a system of 255 solvent molecules and one complex molecule (this corresponds to a density $\rho=0.012$ Å^{-3}), with the temperature fixed at 247 K.

We used a leap-frog Verlet algorithm for both rotations and translations with a time step $\Delta t=0.2$ fs. In our codes we used algorithms from Ref. 23, while for the constant-temperature leap-frog algorithm for rotations we used the scheme suggested in Ref. 24.

As we saw earlier, the intermolecular potentials include a Coulombic part, therefore a decision has to be made about how to treat the long-range forces. Since we want to compare our calculation with those of Sec. III, we followed their treatment: instead of the more usual Ewald summation method, all Coulombic parts in the solvent-solvent and complex-solvent interactions were spherically truncated to zero at $R_c=13.8$ Å, using the smoothing function[25]

$$T(R)=\begin{cases} 1 & \text{if } R<R_T, \\ 1-\dfrac{(R-R_T)^2(3R_c-2R_T-2R)}{(R_c-R_T)^3} & \text{if } R_T\leqslant R\leqslant R_c \\ 0 & \text{if } R_c<R, \end{cases} \tag{4.6}$$

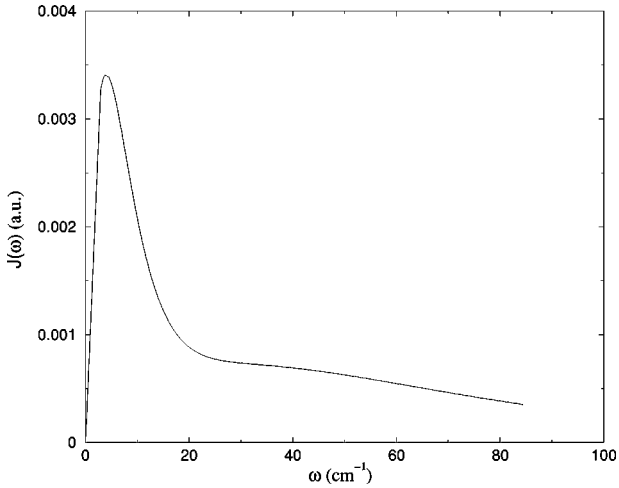

FIG. 2. The spectral density calculated from a molecular dynamics simulation, as discussed in the text. Note that it is peaked at a very low frequency.

where $R_T=0.95R_c$.

The system was equilibrated for 6 ps and then we performed a molecular dynamics run for 14 ps. The long run was necessary to ensure decay of the force-force autocorrelation function. During the MD run the proton was held fixed[3,4,26] at the top of the barrier. For each step of the MD run the total force $F(t)$ on the proton was calculated and stored. Then the dynamical friction $\gamma(t)$ was calculated from the fluctuation-dissipation theorem Eq. (1.2).

Finally the spectral density $J(\omega)$ was calculated by taking the inverse cosine Fourier transform of Eq. (4.2). In Fig. 2 we plot the calculated spectral density, which we have smoothed out with a high order polynomial regression. As can be seen, the spectral density is peaked at very low frequency, a fact that justifies approximating the quantum spectral density by the corresponding classical quantity. In addition, the characteristic time scale of the bath (roughly 2π over the peak frequency of the spectral density) is about 2.5–5 ps. On the other hand, the decay time of the flux autocorrelation function Eq. (4.8) (which determines the rate after the integration Eq. (4.7)) is about 0.25–0.5 ps. This disparity in time scales justifies the expression ''fast proton motion'' we have been using.

B. Quantum calculation

Similarly to our previous work on the quantum Kramers problem, we calculated the reaction rate using the Miller-Schwartz-Tromp formula[27]

$$k=\frac{1}{Q_r}\int_0^{+\infty} dt' C_f(t'), \tag{4.7}$$

where $C_f(t)$ is the flux-flux correlation function

$$C_f(t)=\frac{1}{4m^2}\int dq \int dq' \times\left[\frac{\partial^2}{\partial x\partial x'}|\langle x'q'|e^{-i(H_x+H_q+f\,)t_c}|xq\rangle|^2\right]_{x=x'=0}, \tag{4.8}$$

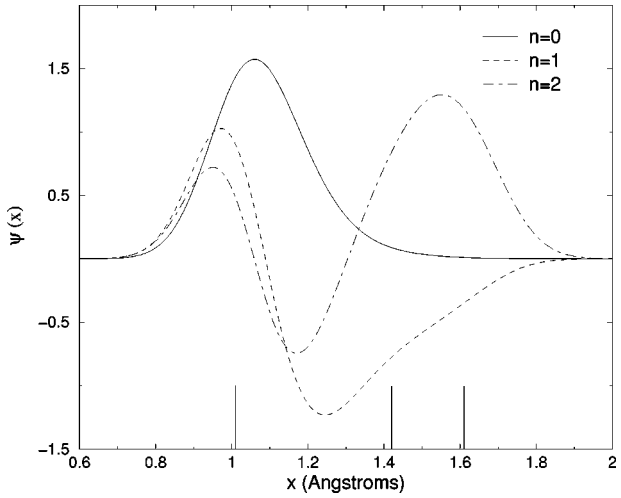

FIG. 3. Eigenfunctions of the potential Eq. (2.2) that is plotted in Fig. 1. The locations of the center of the reactant well, of the transition state and the center of the product well are marked at the bottom of the figure. Note that the ground state, that has an energy well below the other states (see Fig. 1), is localized in the reactant well.

where $t_c = t - i\beta/2$ is the complex time, q is a multidimensional bath coordinate, and $f = cqx$ is the bilinear coupling as shown in Eq. (1.3). The transition state was taken at $x = x' = 0$.

The integrals in Eq. (4.8) can be performed analytically, as we have shown in Ref. 16. We quote the final result:

$$C_f = C_f^0 B_1 Z_{\text{bath}}^{\neq} - \int_0^\infty d\omega \kappa_f^0 J(\omega) B_2(\omega) Z_{\text{bath}}^{\neq}. \tag{4.9}$$

In this equation $J(\omega)$ is the spectral density of the bath, C_f^0 is the correlation function for the *uncoupled* one-dimensional problem, B_1 and B_2 are functions that depend on the characteristics of the bath and on the barrier frequency ω_b (the detailed forms of these functions are given in Ref. 16), $Z_{\text{bath}}^{\neq}$ is the bath partition function when x is at the transition state and

$$\kappa_f^0 = \frac{1}{4m^2} |\langle x=0 | e^{-iH_x t_c} | x=0 \rangle|^2. \tag{4.10}$$

Equation (4.9) is a one-dimensional integral that can be easily calculated numerically and then substituted into Eq. (4.7) for the calculation of the quantum rate. Equation (4.9) shows that whether one uses for the spectral density a simple algebraic form like the Ohmic Eq. (4.3), or a complicated form obtained from a MD simulation, it makes no difference in the complexity of the calculation of the rate.

The exponential resummation technique[15] that we have developed and that led to the result Eq. (4.9), has the advantage that it reduces the calculation of a multi-dimensional propagator to an integral over frequencies and a calculation of the one-dimensional propagator $\langle x' | \exp(-iH_x t) | x \rangle$. As is well-known,

$$\langle x' | e^{-iH_x t} | x \rangle = \sum_n \phi_n(x) \phi_n^*(x') e^{-iE_n t}, \tag{4.11}$$

TABLE II. Comparison of quantum rates as calculated in the present paper and in Refs. 13, 14. As we discussed in Sec. III, a Landau-Zener and a centroid calculation were performed in Ref. 13 and a surface-hopping calculation in Ref. 14. The rates are in s^{-1}.

This work (MFP)	This work (gas-phase)	Ref. 13 (LZ)	Ref. 13 (centroid)	Ref. 14 (MDQT)
0.65×10^9	9.9×10^9	7.8×10^9	10.5×10^9	78×10^9

where ϕ_n, E_n are the eigenstates and eigenvalues of the one-dimensional potential energy surface Eq. (2.2). In order to diagonalize the potential Eq. (2.2) we used the Fourier Grid Hamiltonian method.[28] In this method, one first constructs a grid of equally spaced points and a set of δ-functions centered at the grid points is used as a basis set; this basis constitutes a complete set in the space that consists of the grid points. For the diagonalization of the potential Eq. (2.2) we used a grid of 255 points. In Fig. 3 we have plotted the lowest three eigenfunctions. It is evident from Fig. 3 that the ground state (which lies well below the other states as can be seen in Fig. 2) of such an asymmetric potential is really a ground state harmonic wave function localized in the reactant well.

We show our results in Tables I, II, and III. Table I shows the ratio k/k_{ZPE} of the quantum rate k over the ''semiclassical'' rate k_{ZPE}, which is the TST result corrected for zero-point energy in the reactant well. This ratio gives an indication of the quantum character of the charge transfer. For the present problem k_{ZPE} is equal[13] to 8.6×10^6 s^{-1}.

Table II (which can be obtained from Table I) compares our calculated quantum rate with those of Refs. 13, 14. Our calculation for the H/D kinetic isotope effect (KIE) is shown in Table III. Our results differ from Ref. 14, but they are in reasonable agreement with those of Ref. 13. The reasonableness of the results also shows that the gas phase potential was the correct potential to use in our implementation of the Zwanzig Hamiltonian. The point should be made that in fact the level of agreement between the three calculations should possibly be viewed as rather extraordinary given the completely different approaches taken in the calculations. Quantum calculations of reaction rates in condensed phases for a model as detailed as that used in the three studies were certainly impossible 10 to 15 years ago.

The methods used in Ref. 13 assume that one can average the effect of the bath and produce an effective potential for the reaction coordinate. The spectral density we calculated and is seen in Fig. 2 validates this assumption of adiabatic separation of time scales, since it is peaked at a very low frequency.

TABLE III. Comparison of the H/D kinetic isotope effect as calculated in the present paper and in Refs. 13, 14.

This work (gas-phase)	Ref. 13 (LZ)	Ref. 13 (centroid)	Ref. 14 (MDQT)
83	40	46	3.9

Table II indicates that the quantum enhancement of the rate is very large. It is well known[29] that the KIE measurements tend to be large when large quantum effects are present, a fact that calls into question the small KIE value 3.9, calculated in Ref. 14 (however, as we pointed out earlier[20] it may be possible to reconcile the values of the KIE calculated in Refs. 13, 14). We verified the observation mentioned in Ref. 14, that even when keeping only the lowest 2 proton states the rate calculation has converged. On the other hand, our quantum flux-flux correlation function decayed in about 0.5 ps, while Ref. 14 mentions that when the proton reached the transition state region the time step that was used was equal to 0.001 ps, and if after 10 or more steps the proton returned to the reactant well the procedure was repeated. This suggests a disparity in time scales, but the methods are so different that it is hard to reach any conclusions.

In the last few years there have been quite a few publications[15,30,31] devoted to the study of the quantum Kramers problem, i.e., the quantum equivalent of the Hamiltonian Eq. (1.3). These studies usually assume that the potential energy surface is a quartic double well, or in the case of Ref. 31 that is harmonic in a quantum transition state approximation. This method, like Wolynes' quantum Grote-Hynes method[32] would not be appropriate for the present problem because the product well is so shallow that dynamics within it should be important, a piece of physics that cannot be captured with a harmonic transition state assumption. Both the gas phase and mean field potentials are highly anharmonic near the transition state as seen in Fig. 1.

The objective of these works is to investigate the whole rich dynamical behavior of this system, from friction below to friction above the Kramers turnover and from temperatures below to temperatures above crossover. As we move in this parameter space, different effects may become the dominant mechanism. In order to study the complicated interplay and competition of unrelated dynamical mechanisms, a simple potential and interaction with the bath had to be assumed. However, the methods developed for the study of the quantum Kramers problem are not restricted to a double well potential and a harmonic bath. For example, our result Eq. (4.9) can handle any spectral density as an input and is therefore equally suitable for the study of an anharmonic bath. Finally, we should mention that there is an important physical mechanism that has been omitted from the Azzouzz–Borgis model: an intramolecular oscillation that modifies the proton transfer can have a large effect on the rate, even though it has only marginal importance for the transfer of the much lighter electron. Such oscillations have been called ''rate-promoting'' vibrations by Benderskii and co-workers who studied their effect in gas-phase reactions.[21] Hynes[9] and Silbey[33] have studied the effect of such promoting vibrations in condensed phases in two-level systems, while we have studied[34] the more general case when excitations to higher states are possible (which is the case for proton transfer reactions at room temperature). We have shown[34] how to include this effect in the quantum Kramers problem, but we have left it out in the present study since our objective was to compare the results of our method with those of Refs. 13, 14 using exactly the same model.

The major assumption in this work is that there can be found a hypothetical harmonic bath bilinearly coupled to the reaction coordinate, such that classically it produces the same dynamical friction as the actual anharmonic bath. As we have emphasized repeatedly throughout the paper, this is only possible if the linear Generalized Langevin Equation is a valid approximation. It is known that this is a valid approximation for a large number of systems; we should point out, however, that certain classical MD simulations have shown that this may not always be the case (see Refs. 4, 7, 35 and references cited therein). We are not aware of any quantum rate calculation in condensed phase that has included the effect of a position-dependent friction (equivalently, nonlinear coupling to a harmonic bath). The other assumption that is implicit in the use of a linear GLE, is that the dynamical friction is independent of temperature. Recently, there have been unexpected experimental results[36] that suggest that for certain systems, there are temperature-dependent narrow peaks in the low-frequency part of the spectral density. The origin of this effect merits investigation and microscopically corresponds to the case when the hypothetical bath is bilinearly coupled, but is not harmonic. In another recent publication[37] we have shown that such narrow peaks in the spectral density have a small effect on quantum rate calculations.

ACKNOWLEDGMENTS

It is a pleasure to thank Professors Bruce Berne, Casey Hynes, and Eli Pollak for enlightening remarks about the meaning of the mean-field potential in reaction rate calculations and Professor John Tully for comments on the manuscript. We are grateful to Dr. Peter Gross for providing us with the code for the Fourier grid Hamiltonian method. The authors gratefully acknowledge the support of the chemistry division of the National Science Foundation through Grant No. CHE-9707858. We also acknowledge support of the Office of Naval Research and the NIH.

[1] D. Forster, *Hydrodynamic Fluctuations, Broken Symmetry, and Correlation Functions* (Addison–Wesley, Reading, 1975).
[2] B. J. Berne and G. D. Harp, Adv. Chem. Phys. **17**, 63 (1971).
[3] J. T. Hynes, in *The Theory of Chemical Reaction Dynamics*, edited by M. Baer (CRC, Boca Raton, 1985), Vol. IV, p. 171.
[4] J. B. Strauss and G. A. Voth, J. Chem. Phys. **96**, 5460 (1992).
[5] R. Zwanzig, J. Stat. Phys. **9**, 215 (1973).
[6] R. F. Grote and J. T. Hynes, J. Chem. Phys. **73**, 2715 (1980); **74**, 4465 (1981).
[7] J. E. Straub, M. Borkovec, and B. J. Berne, J. Phys. Chem. **91**, 4995 (1987); J. Chem. Phys. **89**, 4833 (1988); J. E. Straub, B. J. Berne, and B. Roux, *ibid.* **93**, 6804 (1990).
[8] W. Keirsted, K. R. Wilson, and J. T. Hynes, J. Chem. Phys. **95**, 5256 (1991); B. J. Gertner, K. R. Wilson, and J. T. Hynes, *ibid.* **90**, 3537 (1989), and references cited therein.
[9] D. Borgis and J. T. Hynes, J. Chem. Phys. **94**, 3619 (1991).
[10] G. A. Voth, D. Chandler, and W. H. Miller, J. Chem. Phys. **91**, 7749 (1989); G. A. Voth and E. V. Gorman, *ibid.* **94**, 7342 (1990); D. Li and G. A. Voth, J. Phys. Chem. **95**, 10425 (1991).
[11] G. A. Voth, Adv. Chem. Phys. **93**, 135 (1996).
[12] J. C. Tully, J. Chem. Phys. **93**, 1061 (1990).
[13] H. Azzouzz and D. Borgis, J. Chem. Phys. **98**, 7361 (1993).
[14] S. Hammes-Schiffer and J. C. Tully, J. Chem. Phys. **101**, 4657 (1994).
[15] S. D. Schwartz, J. Chem. Phys. **105**, 6871 (1996).
[16] S. D. Schwartz, J. Chem. Phys. **107**, 2424 (1997).

[17] E. R. Lippincott and R. Schroeder, J. Chem. Phys. **23**, 1099 (1955); **23**, 1131 (1955).
[18] B. Bigot, B. J. Costa-Cabral, and J. L. Rivail, J. Chem. Phys. **83**, 3083 (1985).
[19] S. Hammes-Schiffer and J. C. Tully, J. Chem. Phys. **103**, 8528 (1995); D. F. Coker and L. Xiao, *ibid.* **102**, 496 (1995); F. Webster, E. T. Wang, P. J. Rossky, and R. A. Friesner, *ibid.* **100**, 4835 (1994), and references cited therein.
[20] Tully has found that the difference between his results and the Landau-Zener result of Azzouzz–Borgis may be ascribed to differences in the method of calculation of nonadiabatic coupling elements. Apparently, when similarly calculated coupling elements are used, the results of Refs. 13, 14 are in better agreement [J. C. Tully (personal communication)].
[21] V. Benderskii, D. Makarov, and C. Wight, Adv. Chem. Phys. **88**, 1 (1994).
[22] J. S. Bader, R. A. Kuharski, and D. Chandler, J. Chem. Phys. **93**, 230 (1990); N. Makri, E. Sim, D. E. Makarov, and M. Topaler, Proc. Natl. Acad. Sci. USA **93**, 3926 (1996).
[23] M. P. Allen and D. J. Tildesley, *Computer Similation of Liquids* (Clarendon, Oxford, 1987).
[24] D. Fincham, N. Quirke, and D. J. Tildesley, J. Chem. Phys. **84**, 4535 (1986).
[25] O. Steinhauser, Mol. Phys. **45**, 335 (1982).
[26] J. P. Bergsma, B. J. Gertner, and K. R. Wilson, J. Chem. Phys. **86**, 1356 (1987).
[27] W. H. Miller, S. D. Schwartz, and J. W. Tromp, J. Chem. Phys. **79**, 4889 (1983).
[28] C. C. Marston and G. G. Balint-Kurti, J. Chem. Phys. **91**, 3483 (1989).
[29] D. Antoniou and S. D. Schwartz, Proc. Natl. Acad. Sci. USA **94**, 12360 (1997); A. Kohen and J. Klinman, Acc. Chem. Res. **31**, 397 (1998).
[30] M. Topaler and N. Makri, J. Chem. Phys. **101**, 7500 (1994); Y. Georgievskii and E. Pollak, *ibid.* **103**, 8910 (1995).
[31] G. Gershinsky and E. Pollak, J. Chem. Phys. **108**, 2756 (1998).
[32] P. G. Wolynes, Phys. Rev. Lett. **47**, 968 (1981); E. Pollak, Chem. Phys. Lett. **127**, 178 (1986).
[33] A. Suarez and R. Silbey, J. Chem. Phys. **94**, 4809 (1991).
[34] D. Antoniou and S. D. Schwartz, J. Chem. Phys. **108**, 3620 (1998); **109**, 2287 (1998).
[35] E. Neria and M. Karplus, J. Chem. Phys. **105**, 10812 (1996).
[36] A. Passino, Y. Nagasawa, and G. R. Fleming, J. Chem. Phys. **107**, 6094 (1997).
[37] D. Antoniou and S. D. Schwartz, J. Chem. Phys. **109**, 5487 (1998).